Aalborg Universitet

Estimation of combined sewer overflow discharge: a software sensor approach based on local water level measurements

Malte Ahm, Søren Thorndahl, Jesper E. Nielsen and
Michael R. Rasmussen

ABSTRACT

Combined sewer overflow (CSO) structures are constructed to effectively discharge excess water during heavy rainfall, to protect the urban drainage system from hydraulic overload. Consequently, most CSO structures are not constructed according to basic hydraulic principles for ideal measurement weirs. It can, therefore, be a challenge to quantify the discharges from CSOs. Quantification of CSO discharges are important in relation to the increased environmental awareness of the receiving water bodies. Furthermore, CSO discharge quantification is essential for closing the rainfall-runoff mass-balance in combined sewer catchments. A closed mass-balance is an advantage for calibration of all urban drainage models based on mass-balance principles. This study presents three different software sensor concepts based on local water level sensors, which can be used to estimate CSO discharge volumes from hydraulic complex CSO structures. The three concepts were tested and verified under real practical conditions. All three concepts were accurate when compared to electromagnetic flow measurements.

Key words | combined sewer overflow (CSO), computational fluid dynamics (CFD), discharge monitoring and quantification, software sensors, water level measurements

Malte Ahm (corresponding author)
Aarhus Water Ltd.,
Bautavej 1, DK-8210 Aarhus V
Denmark
E-mail: *msa@aarhusvand.dk*

Malte Ahm
Søren Thorndahl
Jesper E. Nielsen
Michael R. Rasmussen
Department of Civil Engineering,
Aalborg University,
Sofiendalsvej 9-11,
DK-9000 Aalborg,
Denmark

INTRODUCTION

Combined sewer overflows (CSOs) contribute significant loads in the form of finer suspended and soluble pollutants to receiving water bodies (Hvitved-Jacobsen *et al.* 2010). Increased environmental awareness of European water bodies have, since the 1970s, resulted in four major European directives (EEC 1976, 1991; EC 2000, 2006) to improve the quality of Europe's water bodies:

- The Bathing Water Directive (76/160/EEC)
- The Urban Waste Water Treatment Directive (91/271/ EEC)
- The Water Framework Directive (2000/60/EC)

- The New Bathing Water Directive (2006/7/EC repealed 76/160/ECC).

Each EU country incorporates the directives into national legislation, and defines methods and means to mitigate the level of pollutants discharged into water bodies. In Denmark, water utilities have to apply for discharge permits, for every overflow structure, at the given municipal authority. These permits are based on static emission requirements from design practices in Denmark. The compliance of these permits is normally based on model simulations and not on actual measurements and environmental assessments of the receiving water body.

Many Danish water utilities are in the process of replacing combined sewers with separated sewers. It is an effective solution to reduce the discharge of pollutants from wastewater into water bodies from CSOs. However,

stormwater can contain pollutants. Thus, treatment of stormwater may be necessary before release to the receiving water body. The process of replacing combined sewers with separated sewers is costly and will take several decades to complete. Meanwhile, continuous monitoring and quantification of CSO discharge loads are highly relevant to mitigate the pollutant loads from existing CSO structures, and comply with the European water directives. Quantification of the actual discharge loads is important to ensure good environmental protection for the capital investment, when renovating and replacing existing drainage systems.

Reliable measurement and prediction of CSO discharge loads can be utilised to mitigate the environmental impact of CSOs, using real-time control (RTC). RTC of urban drainage systems utilises current and predicted states of flows and water levels in the system to adjust the control strategy (Quirmbach & Schultz 2002; Schütze *et al.* 2004; Vanrolleghem *et al.* 2005; Ruggaber *et al.* 2007; Dirckx *et al.* 2011a; Vezzaro *et al.* 2014; Vezzaro & Grum 2014). Thus, it is possible to reduce discharge loads (environmental impact) by actively controlling the urban drainage system (e.g. gates, pumps and basins). Information about the current environmental and hydraulic states of the CSO recipients can also be integrated into RTC strategies (e.g. Vanrolleghem *et al.* 2005; Fu *et al.* 2008; Langeveld *et al.* 2013).

Accurate measurements of CSO emission flows are also important for calibration of urban drainage models used for analyses, etc. Many models are based on mass-balance principles. Hence, it is necessary to have a good knowledge of the boundary conditions: rainfall, inflow to the wastewater treatment plant (WWTP), infiltration, exfiltration, CSO discharge etc., to properly calibrate these urban drainage models.

Continuous monitoring and quantification of CSO discharge loads are rare for non-research purposes. For research purposes, several examples of monitoring programs are found in a number of research studies (Gruber *et al.* 2004, 2005; Gamerith *et al.* 2009; Dirckx *et al.* 2011b; Sharma *et al.* 2014). These earlier studies have focused on measuring pollutant concentrations. To quantify CSO discharge loads, it is necessary to estimate both pollutant concentrations and corresponding water discharge volumes.

Direct measurement of emission flow rates at the weir of a complex CSO structure is practically impossible with current available sensor technology. As a result, CSO structures are usually monitored by simple on/off switches or with water level sensors, if monitored at all. By the use of water level measurements of the upstream hydraulic head, and a standard weir equation (Q-h relation), the upstream

hydraulic head can be translated to an estimate of the emission flow rate (Brorsen & Larsen 2007):

$$Q = C\,L\,h\sqrt{2\,g\,h} \tag{1}$$

where Q [m³/s] is the estimated emission flow rate, C [–] is a coefficient describing the weir crest shape, L [m] is the length of the weir, h [m] is the upstream hydraulic head, and g [m/s²] is the gravitational acceleration. The standard weir equation is valid for hydraulic ideal broad- and sharp-crested weirs with large upstream cross-sections, where the velocity head can be neglected. However, most CSO structures have a complex geometry optimised to effectively discharge excess water within the physical restrictions posed by the surrounding urban environment. Hence, they are usually not designed according to basic hydraulic principles for ideal weirs with a well-defined nappe, and an upstream uniform flow with hydrostatic pressure distribution. Utilising a water level sensor in combination with a standard weir equation for a complex CSO structure can lead to significant errors in the estimated discharge rates and volumes (Fach *et al.* 2009). However, the benefit of utilising water level sensors is that they are cheap and often easy to install in CSO structures.

This study explores and validates how three hydraulic principles can be used to develop software sensors to estimate CSO emission flow rates from complex CSO structures. The generic definition of a software sensor is software that utilises sensor inputs from one or multiple physical sensors to calculate new parameters that are not measured, e.g. utilising water level sensors to calculate flow rates. The definition is broad and has been used differently within different fields. Within the urban drainage field, the software sensor term has, for example, been associated with grey-box modelling (Carstensen *et al.* 1996; Bechmann *et al.* 1999; Carstensen & Harremoës 1999). Leonhardt *et al.* (2012) used the term for a concept based on simple conceptual models where excess flows from all CSO structures in a sewer system were estimated. In the present study, the software sensor term is used in its most direct and simple form: utilising an easily measurable parameter to estimate a difficult measureable parameter via a simple software algorithm. Hence, all developed software sensors in this study are based on local water level measurements. Figure 1 illustrates the three hydraulic principles used to develop the software sensors in this study.

The software sensor concepts developed on the three hydraulic principles (Figure 1) are, in this study, referred to as: basin flow sensor (BFS), channel flow sensor (CFS),
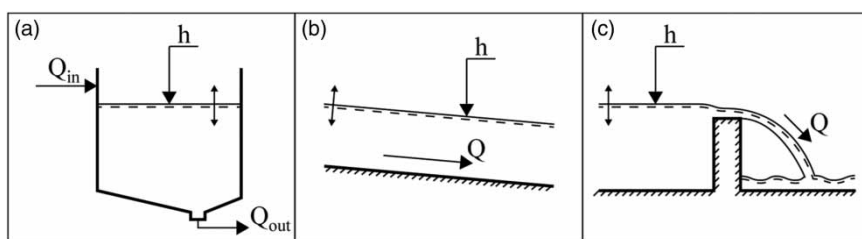
Figure 1 | Three hydraulic principles, which can be utilised to estimate flows on the basis of water level measurements ((a) basin, (b) channel/pipe and (c) weir). Q is the flow and h is the water level.

and weir flow sensor (WFS). All three concepts are based on the principles of Q-h relations from standard hydraulic text-book material. The challenge is to develop and apply Q-h relations to non-ideal and complex CSO structures. The development of the first two software sensor concepts (Figure 1(a) and 1(b)) are based on data-driven Q-h relations estimated on the basis of corresponding water level and flow measurements. The development of the third software sensor (Figure 1(c)) is based on a three-dimensional (3D) computational fluid dynamic (CFD) model of the CSO structure. The first two software sensor concepts in this study are dependent on calibration measurements, whereas the third concept is independent and only based on the physical layout and parameters of the CSO structure. Hence, no cali-bration measurements are needed for the third software sensor concept.

Several authors have used CFD models to estimate the hydraulic behaviour of complex CSO structures (Lipeme Kouyi *et al.* 2003, 2005, 2011; He *et al.* 2006; Vazquez *et al.* 2006; Larsen *et al.* 2008; Fach *et al.* 2009; He & Marsalek 2009; Isel *et al.* 2013, 2014). Lipeme Kouyi *et al.* (2003, 2005), Vazquez *et al.* (2006), He *et al.* (2006), He & Marsalek (2009), and Larsen *et al.* (2008) investigated the hydraulic behaviour of CSO structures by the use of both physical scale models and CFD models. They concluded that CFD models perform at a similar level to physical scale models. However, they also pointed out that, during the setup of a 3D CFD model, it is important to find the optimal spatial and temporal resolutions to obtain accurate results. Lipeme Kouyi *et al.* (2005), Vazquez *et al.* (2006), Fach *et al.* (2009) and Isel *et al.* (2013, 2014) demonstrated the use of CFD models to develop CSO emission flow rate soft-ware sensors based on water level measurements. Fach *et al.* (2009) compared a CFD software sensor (Q-h relation) to standard weir equations and concluded that, for complex CSO structures, the use of standard weir equations may lead to significant deviations in the estimated discharge volume when compared to a CFD software sensor. Isel *et al.* (2014) validated the CFD software sensor methodology

by constructing multiple CFD software sensors based on different combinations of three water level sensors. Unfortu-nately, none of these studies included measurements of actual discharge rates/volumes from full-scale CSO struc-tures to verify the CFD software sensor concept.

The objective of this study was to evaluate the three differ-ent software sensor concepts for hydraulic emission monitoring of CSOs under realistic conditions. A full-scale case study site was used to develop and test the three software sensor concepts against each other, and to obtain actual measurements of discharge volumes. The case site offers a unique possibility to verify the estimated discharge volumes and, thereby, to quantify the quality of these different software sensor concepts under real, practical conditions.

The development of the software sensor concepts was based on the case site. Therefore, the case site, instrumenta-tion of the case site, and available data are presented before the methodology of each software sensor concept.

CASE STUDY SITE, INSTRUMENTATION AND AVAILABLE DATA

The case study site was Viby WWTP in the municipality of Aarhus, Denmark. The catchment area to Viby WWTP con-sists of 678 ha with a combined sewer system and 748 ha with a separated sewer system (Ahm *et al.* 2013). The case study site offers a unique opportunity to close the mass-balance of the case study CSO structure (internal CSO, Figure 2). Figure 2 shows a schematic overview of the over-flow structures at Viby WWTP and the positions of the available hydraulic sensors.

The hydraulic wet weather capacity of Viby WWTP is $1.26 \, \text{m}^3/\text{s}$. When larger runoff flows occur, an internal CSO discharges the excess water to an underground storage basin via an external CSO structure. In these cases, the external CSO functions as a connection channel between the internal CSO and the storage basin. After a CSO event, the stored excess water is pumped back to the
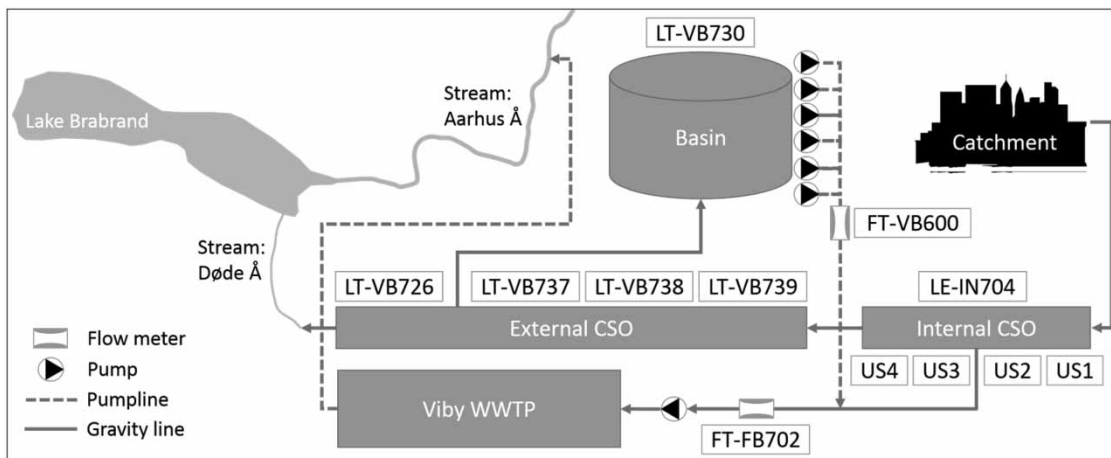
Figure 2 | Schematic overview of the case study site and positions of the hydraulic sensors. The sensors are stated with their internal reference names. Reference abbreviations: FT, flow transmitter; LT and LE, level transmitter; VB, viby basin; IN, inlet; FB, pre-treatment; US, ultrasonic.

WWTP. Thus it is possible to close the mass-balance of the internal CSO, since the discharge volume is measured via the electromagnetic flow meter FT-VB600 when it is pumped back to the WWTP.

The storage basin was inaugurated in September 2011 and has a capacity of approximately 16,000 m³. This capacity corresponds to a rainfall depth of approximately 10 mm for the combined sewer area (runoff contributing area approximately 160 ha). With the construction of the storage basin, Aarhus Water Ltd (water utility) has reduced the number of CSO events at Viby WWTP to the recipient from almost every time it rained to a few times each year. To reduce peak flows from the catchment, basins of varying sizes exist, distributed in the catchment. CSO events in the catchment itself are almost non-existent. Thus, if a CSO occurs it will most likely occur at the WWTP.

Figure 3 shows a 3D visualisation of the internal and external CSO structures, where the physical positions of
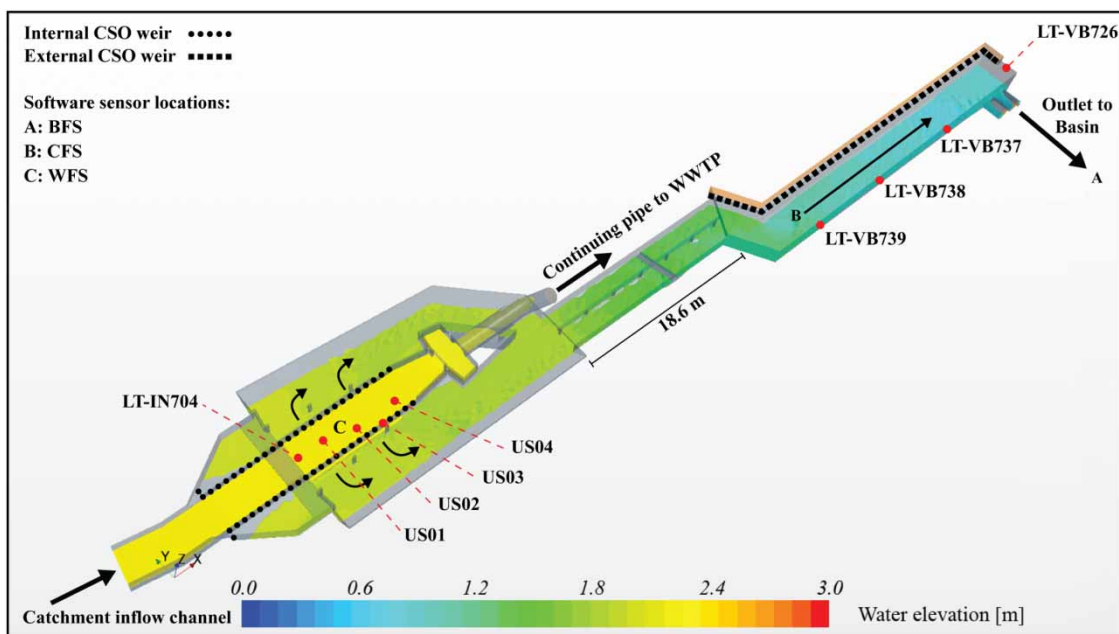
Figure 3 | 3D visualisation of the internal and external CSO structures at Viby WWTP. The locations of the water level sensors in the structures are marked with red. Furthermore, the positions where the software sensors estimate the emission flow rates are also marked. The length of the tunnel connecting the internal and external CSO structures is given to visualise the size of the structures. The water level in the structures is simulated with CFD, with an inlet flow of 2.250 m³/s (internal CSO discharge: 0.990 m³/s).

Table 1 │ Overview of the available hydraulic sensors

Reference	Sensor type	Manufacture/product	Accuracy
LE-IN704	Level (US)	VEGASON 61	±10 mm
LT-VB726	Level (US)	Siemens SITRANS Probe LU	±0.15% FS (6 m)
LT-VB730	Level (P)	Ørum og Jensen SH3102	±0.25% FS (10 m)
LT-VB737	Level (US)	Siemens SITRANS Probe LU	±0.15% FS (6 m)
LT-VB738	Level (US)	Siemens SITRANS Probe LU	±0.15% FS (6 m)
LT-VB739	Level (US)	Siemens SITRANS Probe LU	±0.15% FS (6 m)
FT-VB600	Flow (EM)	Siemens MagFlo 6000	±0.20% MV ± 2.5mm
FT-FB702	Flow (EM)	Siemens MagFlo 6000	±0.20% MV ± 2.5mm
US1[a]	Level (US)	HRLV-MaxSonar®-EZ0™	±1 mm
US2[a]	Level (US)	HRLV-MaxSonar®-EZ0™	±1 mm
US3[a]	Level (US)	HRLV-MaxSonar®-EZ0™	±1 mm
US4[a]	Level (US)	HRLV-MaxSonar®-EZ0™	±1 mm

The sensor principle is stated in parentheses after the sensor type.
US, ultrasonic; P, pressure; EM, electromagnetic; FS, full scale (measurement range); MV, measured value.
[a]Sensors were installed temporarily during the case study period (5th February 2015 to 5th June 2015).

the water level sensors are marked along with the locations where the software sensors estimate the emission flow.

The sensors shown in Figures 2 and 3 are permanently installed in the structures, except for US1, US2, US3, and US4, which were installed temporarily during the case study period to ensure high resolution and quality water level data. Table 1 gives an overview of the sensor types and the manufacturers' specifications of accuracy.

Ultrasonic water level measurements are affected by air density (temperature and humidity). Thus, to obtain very accurate measurements it is necessary to compensate for these changes in air density. The solution, for the high-resolution sensors, was to mount US3 to measure a fixed distance to an aluminium plate. These measurements were used to correct the three other high-resolution sensors (US1, US2 and US4).

The internal CSO structure is a complex, double-sided weir with two different overflow levels and grating, originally built in 1963. The lower weirs are sharp-crested weirs with grating and a facing slope of approximately 37.6°. The upper weirs are concrete walls, which can be defined as broad-crested weirs at low overflow heights, but may act as sharp-crested weirs during large overflow heights due to their narrow width. The length of each side of the lower and upper weirs is approximately 9.35 m and 18.5 m, respectively. The external overflow structure was constructed together with the storage basin, and can be defined as an ideal broad-crested weir with a total length of approximately 39.5 m. Figure 4 shows a photo of the internal and external CSO structures.

The main data period used for evaluation of the software sensors developed in this study was from 5th February 2015 to 5th June 2015. Denmark is located in a temperate coastal climate where heavy rainfall and cloudbursts usually occur from May to September. The data period covers spring and the start of the heavy rainfall season. This period was selected knowingly to ensure that the data contained events where no external CSO would occur. Hence, it would be possible to establish mass-balance since all excess flow would be retained in the basin. Table 2 lists the start and end times of the five CSO events used for the evaluation of the three software sensor concepts.

The calibration of the two data-driven software sensor concepts (BSF and CFS) are based on 12 and 8 calibration events prior to the main data period, respectively. The different numbers of calibration events were due to sensors outages.

SOFTWARE SENSORS AND EVALUATION METHODOLOGY

The unique combination of the basin and CSO structures makes the case site (internal CSO, Figure 2) suitable to test the three different software sensor concepts listed in the introduction: BFS, CFS, and WFS. It is possible to test the software sensors under practical conditions since it is possible to close the mass-balance for most CSO events from the internal CSO structure. For most CSO events, the

Figure 4 | Photograph of the internal and external CSO during dry weather. The left photograph is taken from the north-eastern side of the internal CSO structure. The internal CSO is symmetric along the centreline of the inflow channel. The right photograph is taken from the western side of the external CSO structure.

Table 2 | Start and end times of the five evaluation events used to test the three software sensors

Event no.	Event start time	Event end time
1	4/3/2015 00:20	5/3/2015 01:30
2	26/3/2015 04:00	26/3/2015 19:50
3	12/4/2015 21:00	13/4/2015 18:40
4	3/5/2015 08:30	8/5/2015 10:15
5	18/5/2015 07:45	21/5/2015 01:30

Timestamps are stated in Danish local time (Central European Time with Daylight Saving Time).

whole discharge volume is collected in the basin and pumped back to the WWTP after the CSO event.

The BFS and the CFS are based on Q-h relations obtained from corresponding measurements of water level and flow. It is possible to develop these sensors at this site since the actual discharge volume is measured for most CSOs by the electromagnetic flow meter FT-VB600. However, for practical application of these software sensor concepts at other locations, a temporary measurement campaign for the emission flow rates must be carried out to establish these two CSO discharge software sensors.

The WFS is based on 3D CFD simulations of the overflow structure. The hydraulic behaviour of complex CSO structures is, in principle, similar to ideal measurement weirs. They include a wall where the excess water falls over when the capacity of the continuing pipe is exceeded. Thus, the excess flow reaches a critical flow regime. Consequently, it is possible to formulate a Q-h relation for the given complex CSO structure. However, formulating an accurate Q-h relation theoretical for a complex CSO structure with multiple weirs and grating (to reduce discharge of gross solids) is practically impossible. By the use of CFD it is possible to formulate Q-h relations for different locations in a complex CSO structure based on the physical layout and parameters of the structure.

The evaluation of the three software sensors is based on discharge volumes from the five evaluation events listed in Table 2. The software sensors are compared against measurements from the electromagnetic flow meter FT-VB600, which measures the discharge volume when the basin is emptied via pumps. It is not possible to evaluate the exact emission flow rates, as no measurements of the actual emission flow rates exists, only discharge volumes.

It is important to underline that this study is limited to the internal CSO, since it is only possible to close the mass-balance for this CSO structure. No measurements of the excess flow from the external CSO exist. It has no influence on the relevance of the study, since the scope of the study is to explore and validate the software sensor concepts, and not to estimate the CSO discharge to Lake Brabrand. Hence, the developed software sensors are only valid as long as the external CSO does not overflow and the basin is not full.

Basin flow sensor

The BFS is based on the hydraulic principle illustrated in Figure 1(a). The principle is based on the following mass-balance equation:

$$Q_{in} = \Delta S + Q_{out} \qquad (2)$$

where Q_{in} [m³/s] is the inlet flow to the basin, ΔS [m³/s] is the change in storage volume and Q_{out} [m³/s] is the outlet flow from the basin. Due to the construction layout of the case study site, the inlet flow to the basin is equal to the emission flow from the internal CSO until the basin is full.

The outlet flow from the basin is equal to the pump flow (sensor: FT-VB600) from the basin when it is being emptied. The change in storage is registered as the change in water level (sensor: LT-VB730). Thus it is possible to estimate the inlet flow to the basin via Equation (2), by utilising water level measurements from the basin. However, Equation (2) requires that the geometric relation between the free water surface area and the water level is known, to estimate the change in storage volume. This relation can be based on construction drawings of the basin, but it can also be estimated from corresponding measurements of water level and outlet flow during emptying of the basin ($Q_{in} = 0$).

$$A(h) = \frac{Q_{out} \cdot \Delta t}{\Delta h} \qquad (3)$$

where $A(h)$ [m] is the free water surface area for a given water level (h [m]), Δt [s] is the temporal data resolution, and Δh [m] is the change in water level between two measurements. In this study both construction drawings and Equation (3) were used to develop the BFS. This combination was chosen due to the complex internal layout of the basin. Figure 5 shows the results of the analysis (Equation (3)) along with the fitted model.

The data used for estimating the relation between the free water surface area and water level are scattered slightly around the estimated model. The model is based on linear relations between the seven points listed in Table 3.

The base equation for the BFS is a rewritten version of Equation (2), where the change in storage is assumed to be equal to the inlet flow ($Q_{out} = 0$) and a temporal dimension is added.

$$Q_{in} = \Delta S + Q_{out} \quad \Rightarrow \quad Q_{BFS} = \frac{\Delta h \cdot A(h)}{\Delta t} \quad \Rightarrow$$

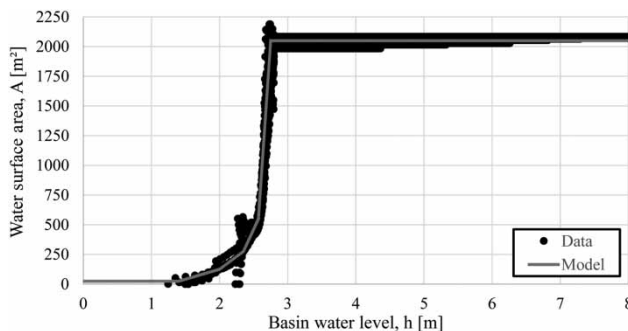$$Q_{BFS} = \frac{(h_t - h_{t-1}) \cdot (a \cdot [\{h_t + h_{t-1}\}/2] + b)}{\Delta t} \qquad (4)$$

Figure 5 │ Estimated relation between the free water surface area and the basin water level. The estimated model is defined in Table 3.

Table 3 │ Model definition of the relation between the free water surface area and the water level

Basin water level [m] (h)	0	1.40	2.00	2.35	2.57	2.75	>2.75
Surface area [m²] (A)	25	25	125	275	550	2,050	2,050

The relations between the points are assumed linear.

where Q_{in} [m³/s] becomes the BFS estimate (Q_{BFS}), t is the given time stamp, Δt [s] is temporal data resolution, and a and b are the slope and intercept, respectively, for the discrete linear model defined in Table 3. The water level was obtained by the physical sensor LT-VB730.

The BFS has two purposes in relation to this study. Firstly, it is an independent software sensor, and secondly it will also act as the flow estimate used to develop the CFS described in the next section.

Channel flow sensor

The CFS is based on the hydraulic principle illustrated in Figure 1(b). The principle is based on the following power-law function:

$$Q_{CFS} = k_1 \cdot h^{k_2} \qquad (5)$$

where Q_{CFS} [m³/s] is the channel flow, h [m] is the water level obtained by the physical water level sensors (LT-VB726, LT-VB737, LT-VB738 and LT-VB739), and k_1 and k_2 are the power law parameters. It is possible to estimate unambiguous Q-h relationships for each water level sensor, since a critical flow regime will occur at the outlet of the inlet pipe to the basin when the basin is not filled. Figure 6 shows the water level measurements obtained in the external CSO channel, and the flow estimates used to estimate the CFSs. The BFS estimate (Equation (4)) is assumed equal to the channel flow.

Based on the scatterplot shown in Figure 6, it was chosen to formulate two CFSs based on sensor LT-726 and LT-VB737, individually. A clear correlation between water level and basin inlet flow exists for these two sensors up to a flow of approximately 3 m³/s. Above this flow level, the data shows a characteristic elliptical shape around the fitted function, representing a classical dynamic wave passing the sensors. However, this elliptical-shaped data is from a single event; hence, the fitted relationship may be representative for flows above 3 m³/s if the flow is
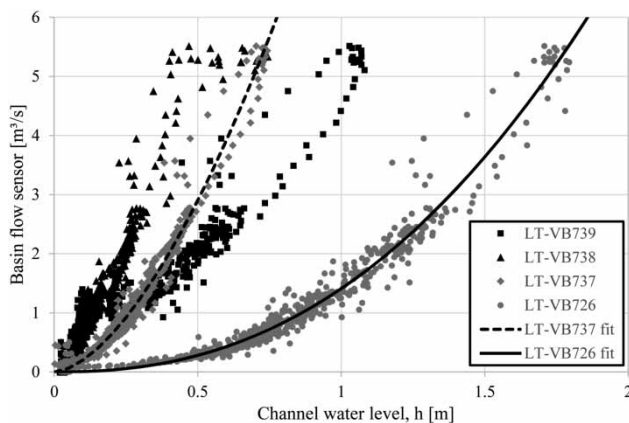
Figure 6 | Scatterplot of water level measurements from the external CSO and BFS estimates. A Q-h relation has been fitted to the relation between LT-VB726 and BFS (Equation (4)) and the relation between LT-VB737 and BFS (Equation (4)) by the use of Equation (5). The R^2 values of the two fits shown are both 0.97.

quasi-stationary. If waves occur, significant uncertainties on the flow rate estimates can be expected since the CFSs will underestimate the flow rate on the front side of the wave and overestimate the flow rate on the back side of the wave. However, if the Q-h fit is a good representation on average, the accumulated volume error will be small since the under- and overestimation will balance each other. The two CFSs based on LT-VB726 and LT-VB737 are entitled CFS A and B, respectively. For equal flows, large differences in water level exist between the two CFSs. This is probably caused by a hydraulic jump between the two sensors due to two changes in the channel slope and a change in flow direction at the basin intake.

It was chosen not to formulate CFSs based on LT-VB738 and LT-739. LT-VB738 has a 'steep' correlation that will result in a less sensitive software sensor compared to LT-726 and LT-VB737. The correlation for LT-VB739 is ambiguous and does not fit a power low function (Equation (5)). The ambiguity is presumably a result of the directional change of the external CSO channel just upstream of the sensor (see Figures 3 and 4).

Weir flow sensor

The WFS is based on the hydraulic principle illustrated in Figure 1(c). The Q-h relation used for the main WFS is obtained from CFD simulations of the CSO structure. Standard weir equations (Equation (1)) are commonly used when modelling urban drainage systems and assessing emission flows from even complex CSO structures. A standard weir equation is, therefore, a good reference for the Q-h relation obtained from the CFD simulations. The Q-h

relation obtained from the CFD simulations and a standard weir equation are hereafter entitled CFD-WFS and SWE-WFS, respectively. SWE-WFS is based on Equation (1) using a shape coefficient, C, equal to 0.40 and a weir length of 18.7 m (Figure 4, left).

The main hydraulic phenomena which make it difficult to use a standard weir equation for the case study CSO are multiple weir levels, grating and non-horizontal water levels. By the use of CFD modelling it is possible to simulate these effects and take them into account. However, the hydraulic phenomenon related to the grating is possibly ambiguous because of the unknown and changing degree of blocking during operation, even in this case where the grating is equipped with automatic cleaning. In this study it was assumed that the mechanical cleaning worked as intended. Visual inspection during the main data period did not reveal any significant blockage.

The CFD-WFS is the only independent CSO discharge software sensor in this study, since no discharge observations are needed for calibration. The Q-h relation is estimated by the use of a 3D CFD model based on the physical layout and surveys of the CSO structure, including parameters such as the concrete roughness height (0.005 m). The quality of the 3D model of the CSO structure is essential for the results of the CFD simulations (e.g. Larsen *et al.* 2008). To ensure the quality, the 3D model used in this study was based on construction drawings along with control measurements of the physical structures. Figure 3 shows a 3D visualisation of CSO structure.

By the use of the CFD model it is possible to determine Q-h relations for different locations in the CSO structure. The flow scenarios in the internal CSO structures can be assumed to be quasi-stationary. Thus, to establish the Q-h relations it is only necessary to simulate a number of different flow scenarios with stationary boundaries. In this case, 30 transient simulations were performed. The inlet flow boundary was varied from 1.3 m³/s to 8.5 m³/s. The continuing flow boundary to the WWTP was 1.26 m³/s (maximum wet weather inflow rate). The remaining boundaries were pressure boundaries.

The CFD simulations were performed in CD-adapco Star-CCM+ Version 9.04.011, using the Reynolds-averaged Navier–Stokes equations (RANS) and a structured mesh. The RANS equations were solved with an implicit unsteady solver using a first-order temporal scheme. A second-order, two-phase segregated volume of fluid model was used to model the water level surface, along with an Eulerian multiphase model and a second-order Menter SST K-omega turbulence model.

The CFD model volume is approximately 1,050 m³. To be able to perform the simulations within a reasonable time-frame (months), the upper limit of elements in the structured mesh was 4 million elements, hence, an average element size of 0.0002625 m³ (approximately 0.065 m isotropic side length). However, to obtain accurate results, a finer mesh is necessary in areas, which has a large influence on the results, for example around weirs, grating, and the water surface. By utilising a desired isotropic mesh size of 0.100 m with a two-layer prism layer (0.033 m), a base mesh of 2.8 million elements was obtained leaving 1.2 million elements for refinement. All areas around the weirs were refined to 0.020 m isotropic elements with a five-layer prism layer (0.033 m). The grating consists of 15×3 mm bars with a spacing of 5 mm. The grating was represented via a physical surrogate model (porous medium) that emulated the energy loss through the grating. The energy loss parameters for the porous medium model were estimated from the grating shape and spacing (Idelchik & Steinberg 2005). Simulations were performed to ensure that the energy loss simulated with the porous medium model corresponded to the energy loss simulated with a physical representation of the grating. To accurately position the water surface, an anisotropic adaptive mesh refinement extension to Star-CCM+ was programmed to refine the mesh in a vertical direction around the water surface. By implementing the anisotropic adaptive mesh refinement, porous medium and static refinement around the weirs, the number of mesh elements varied between 3.7 and 3.9 million through the simulations.

Based on the results from the CFD simulations, Q-h relations can be defined for different locations upstream from the weirs in the internal CSO. As described in the 'Case study site, instrumentation and available data' section (Figure 3), five physical water level sensors exist in the internal CSO. During this study, it was realised that LE-IN704 did not measure correctly. Consequently, it was chosen to base the CFD-WFS on the four high-resolution water level sensors. US3 was used to correct US1, US2, and US4 for measurement variations caused by air density differences. US1 and US4 were used for data quality control of US2. Thus, the Q-h relation (CFD-WFS) was based on the location of sensor US2. The CFD-WFS Q-h relation is shown in Figure 7 along with the Q-h relation for the SWE-WFS.

Figure 7 shows that the Q-h relations for the CFD-WFS and SWE-WFS vary significantly above a water level head of approximately 0.20 m. Above this water level head, the CFD-WFS Q-h relation levels off compared to the SWE-WFS Q-h relation. At this point, the water level head approaches a height corresponding to half the weir height.
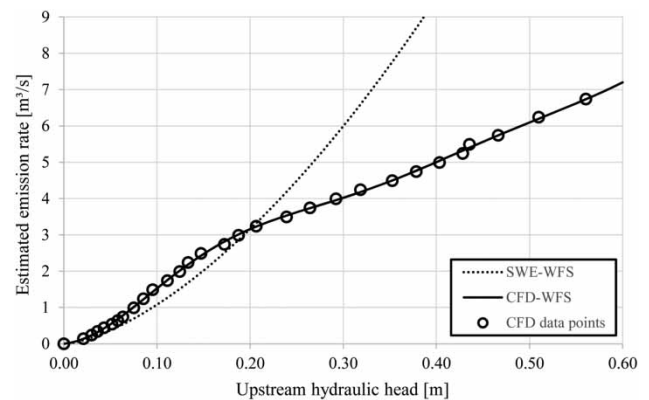

Figure 7 │ Illustration of Q-h relations for CFD-WFS and SWE-WFS. The CFD data points were obtained from the CFD simulations of the CSO structures at the location of the physical sensor US2.

Standard weir equations are usually not valid for higher water level heads (Brorsen & Larsen 2007). Furthermore, at this water level the CFD simulations show that the overflow changes from an overflow weir with a well-defined ventilated nappe to a submerged overflow weir.

RESULTS

Five CSO events from the period 5th February 2015 to 5th June 2015 were used to evaluate the three software sensors described in the 'Software sensors and evaluation methodology' section. Table 2 lists the start and end times of these five events. Figure 8 shows the time series of the physical sensors used for the software sensors during the third evaluation event (12th–13th April 2015) along with the basin inlet flow estimated with the BFS (Equation (4)).

Figure 8 shows that the third CSO event ended at 00:45 13th April 2015 with a basin water level at 5.85 m. Approx. 20 minutes later, the pumps started emptying the basin at a steady rate over the next 17 hours. Notice that the BFS rate is a mirror of the pump flow rate (FT-VB600) during the emptying of the basin. The reason for the mirror is that the BFS is defined positive for inlet flows to the basin, and the pump flow rate (FT-VB600) is defined positive for outlet flows from the basin. Hence, the two flow estimates have opposite operational signs.

Figure 8 shows that the basin sensor should be able to estimate both the inlet and outlet flow of the basin accurately, when compared to the pump flow rate (FT-VB600). If the BFS can estimate the inlet and outlet flow accurately, the volume error should be small when the BFS estimate is integrated for the whole event. Table 4 shows the
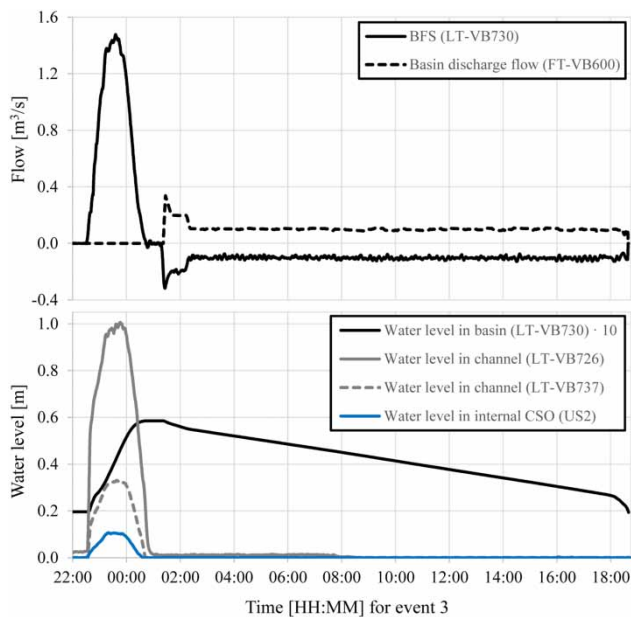
Figure 8 | Time series from event 3 of the physical sensors used for the software sensors shown along with the BFS estimate. The water level measurements from LT-VB730 is scaled with a factor of 10 to fit the graph.

Table 4 | Accumulated discharge volumes estimated with the BFS and integrated volume error (mass-balance) of the BFS when the BFS is used to estimate both inlet and outlet flow to/from the basin

Event no.	BFS [m³]	BFS mass-balance error [m³]
1	5,778	24
2	8,785	−11
3	6,737	8
4*	27,433	2
5*	15,416	−11
Total	64,149	12

The events marked with an asterisk are combined CSO events, where the basin has not been completely emptied before the next event.
BFS, basin flow sensor.

accumulated discharge volume estimated with the BFS, and the integrated volume of the BFS for the whole event as well as for all five evaluation events.

Table 4 shows that the integrated mass-balance error of the BFS for each of the five evaluation events was very small compared to the accumulated discharge volumes estimated with the BFS. The largest mass-balance error is 0.5% (event 1). Tables 5 and 6 show the results from the volumetric evaluation of the software sensors. As a reference, the discharge volume estimated with a standard weir equation (SWE-WFS) is also listed in the tables.

Table 5 | Accumulated discharge volumes for each event for each software sensor

Event no.	EFM [m³]	BFS [m³]	CFS A [m³]	CFS B [m³]	CFD-WFS [m³]	SWE-WFS [m³]
1	5,721	5,778	5,634	5,728	5,658	4,077
2	8,610	8,785	8,764	9,042	8,550	6,301
3	6,600	6,737	6,713	6,965	6,950	4,916
4*	27,049	27,433 (5,355)	5,349	5,563	5,253	3,656
5*	15,808	15,416 (11,600)	11,448	11,652	11,935	8,454
Total	63,788	64,149 (38,255)	37,908	38,950	38,346	27,404

The events marked with an asterisk are combined CSO events where the basin has not been completely emptied before the next CSO. For these events, only the first CSO is used to estimate the CFS A, CFS B, CFD-WFS and SWE-WFS discharge volumes. For BFS, the discharge volume of the first CSO in these combined CSO events is stated in parentheses.
EFM, electromagnetic flow meter (FT-VB600); BFS, basin flow sensor; CFS, channel flow sensor; CFD-WFS, computation fluid dynamic weir flow sensor; SWE-WFS, standard weir equation weir flow sensor.

Table 6 | Deviations in per cent for the estimated discharge volumes compared to EFM discharge volumes (stated in Table 5)

Event no.	BFS [%]	CFS A [%]	CFS B [%]	CFD-WFS [%]	SWE-WFS [%]
1	1.00	−1.52	0.12	−1.10	−28.74
2	2.03	1.79	5.02	−0.70	−26.82
3	2.08	1.71	5.53	5.30	−25.52
4*	1.42	−0.11	3.88	−1.90	−31.73
5*	−2.48	−1.31	0.45	2.89	−27.12
Total	0.57	−0.91	1.82	0.24	−28.36

For the events marked with an asterisk, CFS A, CFS B, CFD-WFS and SWE-WFS were evaluated against the BFS discharge estimates stated in parentheses in Table 5.
BFS, basin flow sensor; CFS, channel flow sensor; CFD-WFS, computation fluid dynamic weir flow sensor; SWE-WFS, standard weir equation weir flow sensor.

The discharge volumes estimated with the BFS corresponded well to the measured discharge volumes (EFM), even for the combined CSO events (four and five). The last two events listed in Table 5 are combined CSO events that consisted of multiple subsequent CSOs where the basin had not been completely emptied before the next event, and backwater effects had occurred from the basin back to the external and internal CSO. As such, the conditions for the BFS, CFSs, CFD-WFS and SWE-WFS were not valid due to the backwater effects. However, the BFS estimate corresponded well to EFM for the last two events. Only the first CSO in the combined CSO events was used to evaluate the CFSs, CFD-WFS and SEW-WFS. The BFS estimate acted as a substitute for EFM for event

four and five since the EFM cannot measure independent CSOs in combined CSO events. Table 6 lists the volumetric deviations between the estimated discharge volume and reference measurements.

Tables 5 and 6 show that the combined volumetric deviations were lowest for the BFS and CFD-WFS. However, for single events, a deviation of approximately 2% and 5% can be observed, respectively. Both CFSs performed very well, whereas SWE-WFS underestimated the discharge volumes significantly. A lower performance of the SWE-WFS was expected due to the complex geometry of the CSO structure.

As described earlier, no measurements exist of the actual CSO emission flow rates, only discharge volumes. However, the BFS corresponds well to the flow rate measurements obtained from the electromagnetic flow meter (Figure 8) when the basin is emptied, and the mass-balance error of the BFS is small (Table 4). Thus, the BFS can be used to assess the dynamic quality of the other software sensors. Figure 9 shows the flow time series estimated with the software sensors for the third evaluation event, along with the flow time series estimate with the SWE-WFS.

The flow time series of the four software sensors and SWE-WFS have a similar shape. However, the maximum level varies within 0.5 m³/s, which corresponds to approximately one-third of the maximum flow estimated with BFS. The two CFSs correspond best to the BFS. However, a good correlation between these sensors was expected since they were developed (calibrated) on corresponding data. The CFD-WFS and SWE-WFS are independent in relation to calibration. SWE-WFS generally underestimates the flow during the whole time series, which corresponds well to the results listed in Table 6. CFD-WFS underestimates slightly in the beginning of the event, overestimates in the middle of the event and underestimates again in the end of the

event. Even though the dynamics did not correspond completely to the BFS, the accumulated discharge volumes corresponded well (Table 6). It should be underlined that no measurements of the actual discharge rates exist. Hence, it cannot be concluded if the dynamics of the BFS was more correct than the dynamics of the CFD-WFS. Both estimates are plausible since the estimated discharge volume corresponds to the measured discharge volume.

DISCUSSION

The two data-driven software sensor concepts were developed by utilising correlation analyses between physical water level sensors and discharge measurements. To utilise this methodology on other CSO structures, where discharge rates/volumes are not measured, a temporary measurement campaign must be conducted to establish the relation. If it is possible to perform a temporary measurement campaign to establish the relation, this study has shown that it is possible to obtain very good results using those types of software sensors. The improvement is significant when compared to standard weir equations. However, if discharge measurements are available, it should be possible to adjust a standard weir equation to perform better than shown in this study. By utilising a shape coefficient, C, of 0.575 instead of the standard ($C = 0.40$) the total deviation becomes less than 1% for the five evaluation events.

The CFD-WFS is the only independent software sensor in relation to calibration in this study. It did not require any calibration to observations to develop the Q-h relation. The Q-h relation is solely based on the CFD simulations of the physical structure in 3D. The distance between the sensor and weir elevations has been measured onsite, and used directly to estimate the hydraulic head needed for the Q-h relation. Small biases in the actual elevations of the sensor and weir could result in large deviations in the estimated emission flow rates due to the length of the weirs. Thus, a small change in water level results in a large change in emission flow rate (Figure 7). This fact contributed to the choice of basing the CFD-WFS on the high-resolution ultrasonic water level sensors in the internal CSO. The standard water level sensor (IN-LE704) has an accuracy of ±10 mm, whereas the high-resolution sensors have an accuracy of ±1 mm. By the use of the CFD-WFS Q-h relation, the emission flow rate is estimated as 1.53 m³/s for a water level head of 0.1 m. However, by applying the uncertainty of IN-LE704, the emission flow rate could be between 1.319 m³/s and 1.731 m³/s (water
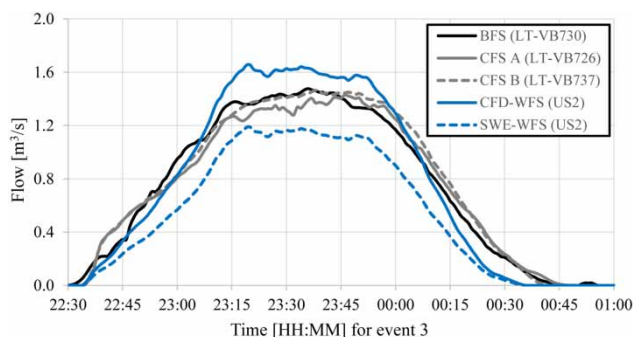
Figure 9 | Flow time series estimated with the software sensors and SWE-WFS for evaluation event 3.

level head 0.09 m and 0.11 m). Thus, the flow rate uncertainty related to the water level measurement is approximately $\pm 0.2 \text{ m}^3/\text{s}$ at a flow rate of 1.53 m^3/s. By utilising the high-resolution water level sensor, this uncertainty is reduced to approximately $\pm 0.02 \text{ m}^3/\text{s}$.

To utilise the CFD-WFS concept properly, it is very important to have a good 3D model of the physical structure, precise measurements of the sensor locations, and accurate sensors that are installed correctly. If these requirements cannot be fulfilled, the CFD-WFS estimates can deviate significantly from the real discharge due to insufficient accuracy in the model description and data. In these cases it may be more beneficial to utilise data-driven software sensors, if it is possible to conduct a temporary measurement campaign.

This study has shown that software sensors based on physically unambiguous and inexpensive sensors can be used, with advantages, to estimate discharge volumes from complex CSO structures that would otherwise be difficult to estimate. Furthermore, multiple physical sensors can be used in combination to improve the robustness of the software sensor system, as described by Isel *et al.* (2014).

Lastly, it is important to underline that the scope of this study was not to estimate the CSO discharge to Lake Brabrand. It was to explore and validate the software sensor concepts under controlled circumstances. Hence, only internal overflows where measurements of the excess flows existed were used. The authors are confident that the CFD software concept can be utilised to estimate the external CSO discharge. It has not been investigated further in this study since no measurements exist to validate it.

CONCLUSION

Three different software sensor concepts for quantification of discharge volumes from complex CSO structures were developed and tested under practical conditions at Viby WWTP in Aarhus, Denmark. The CSO structure used for this study is a complex CSO with multiple weirs and grating. The case site is unique since it is possible to close the mass-balance of the CSO structure and verify the discharge volumes. The discharge volumes were measured via electromagnetic flow meters. These direct discharge measurements were used to evaluate the quality of the software sensor concepts. The evaluation was based on five CSO events recorded during the spring of 2015.

The first two software sensor concepts were based on data-driven Q-h relations between physical water level

sensors and discharge measurements. As such, these sensors need to be calibrated to actual measurements before they can be used to estimate the CSO discharge. The third software sensor concept was based on CFD simulations of the physical layout of the CSO structures. This software sensor is an independent software sensor, which does not need any calibration to discharge measurements.

All three software concepts have proven very accurate when compared to actual measurements of the discharge volumes. The volumetric deviation between discharge measurements and the software sensors was smaller than 2% in total for all evaluation events. However, deviations of approximately 5% were observed for single events. When a standard weir equation is used to estimate the discharge volumes, the volumetric deviations are up to 32%. Hence, all tested software sensors are a significant improvement compared to standard weir equations.

This study has shown that it is possible to develop specific software sensors (Q-h relations) for a complex CSO structure with multiple weirs and grating, and use these software sensors to obtain accurate estimates of the discharge volumes. Furthermore, this study has shown that the CFD-obtained Q-h relation can be used without any calibration to estimate discharge volumes accurately. Software sensors can be implemented at any CSO structure to quantify the emission flow rates and thereby improve the awareness of the actual discharges. Furthermore, the methodologies in this study are not limited to combined sewer systems. They can be applied in any fields of water management.

The Q-h relations obtained from the software sensor concepts tested in this study are simple and can easily be implemented in urban drainage models to ensure a more correct model representation of complex CSO structures. A more correct model representation of complex CSOs will improve the boundary conditions and rainfall-runoff mass-balance. However, this aspect was not investigated further in this study.

ACKNOWLEDGEMENTS

REFERENCES

Ahm, M., Thorndahl, S., Rasmussen, M. R. & Bassø, L. 2013 Estimating subcatchment runoff coefficients using weather radar and a downstream runoff sensor. *Water Science and Technology* **68** (6), 1293–1299. DOI: http://dx.doi.org/10.2166/wst.2013.371.

Bechmann, H., Nielsen, M. K., Madsen, H. & Kjølstad Poulsen, N. 1999 Grey-box modelling of pollutant loads from a sewer system. *Urban Water* **1** (1), 71–78. DOI: http://dx.doi.org/10.1016/S1462-0758(99)00007-2.

Brorsen, M. & Larsen, T. 2007 *Lærebog i Hydraulik*. Aalborg University, Aalborg, Denmark.

Carstensen, J. & Harremoës, P. 1999 Gray-box modeling approach for description of storage tunnel. *Journal of Hydraulic Engineering* **125** (1), 17–25. DOI: http://dx.doi.org/10.1061/(ASCE)0733-9429(1999)125:1(17).

Carstensen, J., Harremöes, P. & Strube, R. 1996 Software sensors based on the grey-box modelling approach. *Water Science and Technology* **33** (1), 117–126. DOI: http://dx.doi.org/10.1016/0273-1223(96)00164-3.

Dirckx, G., Schütze, M., Kroll, S., Thoeye, C., De Gueldre, G. & Van De Steene, B. 2011a Cost-efficiency of RTC for CSO impact mitigation. *Urban Water Journal* **8** (6), 367–377. DOI: http://dx.doi.org/10.1080/1573062X.2011.630092.

Dirckx, G., Thoeye, C., De Gueldre, G. & Van De Steene, B. 2011b CSO management from an operator's perspective: a step-wise action plan. *Water Science and Technology* **63** (5), 1044–1052. DOI: http://dx.doi.org/10.2166/wst.2011.288.

EC 2000 Directive 2000/60/EC establishing a framework for community action in the field of water policy. *Official Journal of the European Communities* **43** (L 327), 1–73.

EC 2006 Directive 2006/7/EC concerning the management of bathing water quality and repealing directive 76/160/EEC. *Official Journal of the European Union* **49** (L 64), 37–51.

EEC 1976 Council directive 76/160/EEC concerning the quality of bathing water. *Official Journal of the European Economic Community* **19** (L 31), 1–7.

EEC 1991 Council directive 91/271/ECC concerning urban waste water treatment. *Official Journal of the European Economic Community* **34** (L 135), 40–52.

Fach, S., Sitzenfrei, R. & Rauch, W. 2009 Determining the spill flow discharge of combined sewer overflows using rating curves based on computational fluid dynamics instead of the standard weir equation. *Water Science and Technology* **60** (12), 3035–3043. DOI: http://dx.doi.org/10.2166/wst.2009.752.

Fu, G., Butler, D. & Khu, S.-T. 2008 Multiple objective optimal control of integrated urban wastewater systems. *Environmental Modelling & Software* **23** (2), 225–234. DOI: http://dx.doi.org/10.1016/j.envsoft.2007.06.003.

Gamerith, V., Muschalla, D., Könemann, P. & Gruber, G. 2009 Pollution load modelling in sewer systems: an approach of combining long term online sensor data with multi-objective auto-calibration schemes. *Water Science and Technology* **59** (1), 73–79. DOI: http://dx.doi.org/10.2166/wst.2009.772.

Gruber, G., Winkler, S. & Pressl, A. 2004 Quantification of pollution loads from CSOs into surface water bodies by means of online techniques. *Water Science and Technology* **50** (11), 73–80.

Gruber, G., Winkler, S. & Pressl, A. 2005 Continuous monitoring in sewer networks: an approach for quantification of pollution loads from CSOs into surface water bodies. *Water Science and Technology* **52** (12), 215–223.

He, C. & Marsalek, J. 2009 Hydraulic optimization of a combined sewer overflow (CSO) storage facility using numerical and physical modeling. *Canadian Journal of Civil Engineering* **36** (2), 363–373. DOI: http://dx.doi.org/10.1139/S08-050.

He, C., Marsalek, J., Rochfort, Q. & Krishnappan, B. G. 2006 Case study: refinement of hydraulic operation of a complex CSO storage/treatment facility by numerical and physical modeling. *Journal of Hydraulic Engineering* **132** (2), 131–139. DOI: http://dx.doi.org/10.1061/(ASCE)0733-9429(2006)132:2(131).

Hvitved-Jacobsen, T., Vollertsen, J. & Nielsen, A. 2010 *Urban and Highway Stormwater Pollution*. CRC Press, Boca Raton, FL, USA.

Idelchik, I. E. & Steinberg, O. 2005 *Handbook of Hydraulic Resistance*. Jaico Publishing House, Mumbai, India.

Isel, S., Dufresne, M., Bardiaux, J. B., Fischer, M. & Vazquez, J. 2013 Computational fluid dynamics based assessment of discharge-water depth relationships for combined sewer overflows. *Urban Water Journal* **11** (8), 631–640. DOI: http://dx.doi.org/10.1080/1573062X.2013.806561.

Isel, S., Dufresne, M., Fischer, M. & Vazquez, J. 2014 Assessment of the overflow discharge in complex CSO chambers with water level measurements – on-site validation of a CFD-based methodology. *Flow Measurement and Instrumentation* **35**, 39–43. DOI: http://dx.doi.org/10.1016/j.flowmeasinst.2013.11.003.

Langeveld, J. G., Benedetti, L., de Klein, J. J. M., Nopens, I., Amerlinck, Y., van Nieuwenhuijzen, A., Flameling, T., van Zanten, O. & Weijers, S. 2013 Impact-based integrated real-time control for improvement of the Dommel River water quality. *Urban Water Journal* **10** (5), 312–329. DOI: http://dx.doi.org/10.1080/1573062X.2013.820332.

Larsen, T., Nielsen, L., Jensen, B. & Christensen, E. D. 2008 Numerical 3-D modelling of overflows. In: *11th International Conference on Urban Drainage*, pp. 1–7.

Leonhardt, G., Fach, S., Engelhard, C., Kinzel, H. & Rauch, W. 2012 A software-based sensor for combined sewer overflows. *Water Science and Technology* **66** (7), 1475–1482. DOI: http://dx.doi.org/10.2166/wst.2012.331.

Lipeme Kouyi, G., Vazquez, J. & Poulet, J. B. 2003 3D free surface measurement and numerical modelling of flows in storm overflows. *Flow Measurement and Instrumentation* **14** (3), 79–87. DOI: http://dx.doi.org/10.1016/S0955-5986(03)00011-6.

Lipeme Kouyi, G., Vazquez, J., Gallin, Y., Rollet, D. & Sadowski, A. G. 2005 Use of 3D modelling and several ultrasound sensors to assess overflow rate. *Water Science and Technology* **51** (2), 187–194.

Lipeme Kouyi, G., Bret, P., Didier, J. M., Chocat, B. & Billat, C. 2011 The use of CFD modelling to optimise measurement of overflow rates in a downstream-controlled dual-overflow

structure. *Water Science and Technology* **64** (2), 521–527. DOI: http://dx.doi.org/10.2166/wst.2011.162.

Quirmbach, M. & Schultz, G. A. 2002 Comparison of rain gauge and radar data as input to an urban rainfall-runoff model. *Water Science and Technology* **45** (2), 27–33.

Ruggaber, T. P., Talley, J. W. & Montestruque, L. A. 2007 Using embedded sensor networks to monitor, control, and reduce CSO events: a pilot study. *Environmental Engineering Science* **24** (2), 172–182. DOI: http://dx.doi.org/10.1089/ees.2006.0041.

Schütze, M., Campisano, A., Colas, H., Schilling, W. & Vanrolleghem, P. A. 2004 Real time control of urban wastewater systems – where do we stand today? *Journal of Hydrology* **299** (3–4), 335–348. DOI: http://dx.doi.org/10.1016/j.jhydrol.2004.08.010.

Sharma, A. K., Lynggaard-Jensen,,, A., Vezzaro, L., Andersen, S. T., Brodersen, E., Eisum, N. H., Snediker Jacobsen, B., Høgh, J., Gadegaard, T. N., Mikkelsen, P. S. & Rasmussen, M. R. 2014 Advanced monitoring of combined sewer overflows:

what to measure and how to measure. In: *Proceedings of the 13th International Conference on Urban Drainage*.

Vanrolleghem, P., Benedetti, L. & Meirlaen, J. 2005 Modelling and real-time control of the integrated urban wastewater system. *Environmental Modelling & Software* **20** (4), 427–442. DOI: http://dx.doi.org/10.1016/j.envsoft.2004.02.004.

Vazquez, J., Kouyi, G. L. & Zug, M. 2006 Modelling and instrumentation of the storm overflows of the combined sewer system of Sélestat. *Urban Water Journal* **3** (2), 91–110. DOI: http://dx.doi.org/10.1080/15730620600855936.

Vezzaro, L. & Grum, M. 2014 A generalised dynamic overflow risk assessment (DORA) for real time control of urban drainage systems. *Journal of Hydrology* **515**, 292–303. DOI: http://dx.doi.org/10.1016/j.jhydrol.2014.05.019.

Vezzaro, L., Christensen, M. L., Thirsing, C., Grum, M. & Mikkelsen, P. S. 2014 Water quality-based real time control of integrated urban drainage systems: a preliminary study from Copenhagen, Denmark. *Procedia Engineering* **70**, 1707–1716. DOI: http://dx.doi.org/10.1016/j.proeng.2014.02.188.